ADVANCES IN ATMOSPHERIC SCIENCES, VOL. 30, NO. 2, 2013, 397–410

# Revisiting the Climatology of Atmospheric Blocking in the Northern Hemisphere

Ho Nam CHEUNG[1,2], ZHOU Wen*[1,2] (周 文), Hing Yim MOK[3], Man Chi WU[3], and Yaping SHAO[4]

[1] *City University of Hong Kong Shenzhen Research Institute, Shenzhen* 518057

[2] *Guy Carpenter Asia-Pacific Climate Impact Centre, School of Energy and Environment, City University of Hong Kong, Hong Kong*

[3] *Hong Kong Observatory, Hong Kong*

[4] *Institute for Geophysics and Meteorology, University of Cologne, Cologne, Germany*

(Received 6 January 2012; revised 29 May 2012)

**ABSTRACT**

In addition to the occurrence of atmospheric blocking, the climatology of the characteristics of blocking events, including duration, intensity, and extension, in four seasons over the Northern Hemisphere was analyzed for the period 1950–2009. The seasonality and spatial variations of these characteristics were studied according to their longitudinal distributions. In general, there were sharp discrepancies in the blocking characteristics between winter and summer, and these differences were more prominent over the Atlantic and Pacific Oceans. The blocking not only occurred more frequently but also underwent stronger amplification in winter; likewise, the blocking occurred less frequently and underwent weaker amplification in summer. There are very strong interrelationships among different blocking characteristics, suggesting that they are supported by similar physical factors.

In addition, the relationship between blocking over different regions and East Asian circulation was examined. Ural–Siberia is a major blocking formation region in all seasons that may exert a downstream impact on East Asia. The impact is generally weak in summer, which is due to its lower intensity and smaller duration. However, the extratropical circulation over East Asia in summer can be disturbed persistently by the frequent occurrence of blocking over the Asian continent or the Western Pacific. In particular, the blocking frequency over the Western Pacific significantly increased during the study period. This climatological information provides a background for studying the impact of blocking on East Asian circulation under both present and future climate conditions.

**Key words**: atmospheric blocking, climatology, seasonality, East Asian circulation

**Citation**: Cheung, H. N., W. Zhou, H. Y. Mok, M. C. Wu, and Y. Shao, 2013: Revisiting the climatology of atmospheric blocking in the Northern Hemisphere. *Adv. Atmos. Sci.*, **30**(2), 397–410, doi: 10.1007/s00376-012-2006-y.

## 1. Introduction

Atmospheric blocking potentially triggers various climate extremes over the extratropics, which can be extended toward the subtropical region. Climatologically, the westerly jet circulates around the extratropical region; this is called zonal-type circulation. Occasionally, the jet is split and its speed slows down such that the normal atmospheric flow appears to be "blocked". Typical blocking is composed of a barotropic high pressure center and a surface frontal zone (Treidl et al., 1981). While warmer air masses comprise its upstream portions, colder air masses constitute its downstream portions. Long periods of such a quasi-stationary state persistently maintain the meridional flow driving north–south air mass

*Corresponding author: ZHOU Wen, wenzhou@cityu.edu.hk

and energy exchange. This may trigger extreme climate events, such as heat waves, cold waves, drought, and flooding. Two opposite extremes may occur simultaneously at its different components. For example, wildfires in the Ural Mountains, heat waves in Russia, and severe flooding in Pakistan during summer 2010 were the consequences of a long duration of blocking in the vicinity of the Ural Mountains (Dole et al., 2011; Matsueda, 2011; Lau and Kim, 2012).

The enormous impacts of blocking have drawn ample attention to the study of its climatological features for decades (e.g., Rex, 1950). In general, blocking tends to occur at the exit region of a storm track. Over the Northern Hemisphere, the Atlantic Ocean–European Continent, the Pacific Ocean, and the Ural Mountains are three major blocking sectors observed on an annual basis. They are located downstream of the climatological storm tracks over the two open oceans and the Mediterranean Sea (e.g., Barriopedro et al., 2006; Diao et al., 2006; Tyrlis and Hoskins, 2008a). Storm activities act to export warm and anticyclonic fluxes that are favorable for the establishment and maintenance of blocking. Blocking activity may be affected by the position and strength of a storm track (Tyrlis and Hoskins, 2008b; Woollings et al., 2008; Luo et al., 2010b). Because the thermodynamic background varies from season to season, blocking activities and their geographic locations exhibit seasonal variations. Oceanic blocking is more active during cold seasons when the ocean is warmer than the continent, and continental blocking is more active during warm seasons when the continent is warmer than the ocean. However, the impact of blocking on regional climate can be pronounced throughout the year, including but not limited to East Asia.

In the boreal winter, the blocking originating from both Eurasia and the Western Pacific may enhance East Asian winter monsoon (EAWM) activities (Takaya and Nakamura, 2005). As early as the 1950s, the decay of a blocking ridge in the vicinity of the Ural Mountains was known to be followed by an intrusion of intense cold air masses into China (Tao, 1957). Associated with the eastward propagation of a quasi-stationary Rossby wave packet, the maintenance of Ural blocking persistently reinforces the Siberian high to initiate cold air outbreaks in East Asia (Nakamura et al., 1997). In addition to a stronger EAWM (Cheung et al., 2012a), this may result in abnormally long-lasting cold periods, such as that of early 2008 (Zhou et al., 2009). Whereas the EAWM and cold surge activities undergo a substantial weakening trend (Hong et al., 2008; Wang et al., 2009; Hung and Kao, 2010; Wei et al., 2011; Huang et al., 2012), Wang et al. (2010) showed that less blocking near the Ural Mountains is accompanied by more planetary wave activity propagating equatorward, which is likely to be responsible for warmer East Asian winter climate (Chen et al., 2005).

On the other hand, the geographic location of blocking in the boreal summer is quite different from other seasons. In summer, as mentioned previously, continental blocking occurs more frequently. In addition to the Ural Mountains, another blocking center is located near the Sea of Okhotsk. In addition, there is substantial blocking activity in the vicinity of the Lake of Baikal over the Asian continent (Li and Ding, 2004). Summer blocking over East Asia and the Western Pacific may bring substantial cooling to northeastern China, Korea, and northern Japan, as well as affecting the persistence and meridional movement of the meiyu/baiu front (Wang, 1992). On an annual basis, Barriopedro et al. (2006) reported that blocking frequency over Eurasia may exhibit a remarkable decreasing trend while over Western Pacific it may undergo an increasing trend. Accordingly, it is difficult to determine whether the variability of blocking occurrences over the Northern Hemisphere affects East Asian circulation in both summer and winter.

Apart from the occurrence of blocking, the impact of blocking may also be related to the temporal characteristics of an individual blocking event, such as duration, intensity, and extension. In this we investigated the scope of the impact of blocking on East Asia from a climatologic point of view. The impacts can be contributed by both upstream and downstream blocking events; therefore, the climatology of blocking over the Northern Hemisphere was revisited. In the following analysis, the method for detecting blocking is introduced in section 2. Then section 3 presents the climatology of blocking frequency, including the locations of genesis and decay. Sections 4 and 5 focus on the impacts of blocking on East Asia in winter and summer, respectively. Section 6 describes the climatology of different temporal characteristics of blocking events. Finally, a discussion is presented in section 7 followed by a summary in section 8.

## 2. Detection of blocking

Although there is no consensus on the definition of atmospheric blocking, it is necessary to set criteria for a quantitative analysis of blocking. Long-term global reanalysis datasets provide a convenient way to objectively define a blocking index. Previous studies have proposed several ways to define blocking, which were reviewed in detail by Barriopedro et al. (2010). One commonly used blocking index was obtained from the zonal index (Lejenäs and Øakland, 1983; Tibaldi

and Molteni, 1990; Anderson, 1993; Lupo and Smith, 1995; Wiedenmann et al., 2002; Barriopedro et al., 2006; CPC[a]), which can be defined as the north–south gradient of the geopotential height at the 500-hPa isobaric level ($Z_{500}$):

$$\frac{Z_{500}(\phi_{\rm N}) - Z_{500}(\phi_{\rm S})}{\phi_{\rm N} - \phi_{\rm S}} ,$$

where $\phi_{\rm N}$ and $\phi_{\rm S}$ represent the latitude at the north and the south, respectively.

In this study, the National Centers for Environmental Prediction-National Center for Atmospheric Research (NCEP-NCAR) reanalysis datasets (grid resolution 2.5°×2.5°) from April 1950 to March 2010 were extracted (Kalnay et al., 1996). The blocking event algorithm principally follows the one used by Barriopedro et al. (2006), which is applied to the daily field of the $Z_{500}$. Typical blocking is composed of a ridge near 60°N and a low-pressure cell to the south of 40°N (Austin, 1980) such that it has a negative geopotential height gradient in its northern part (ZGN) and a positive geopotential height gradient in its southern part (ZGS). Because the blocking center is a closed high, it should contain a positive anomaly in the time-varying field of the $Z_{500}$. Accordingly, a simple and useful blocking criterion can be determined using the following three equations at each longitude grid point ($\lambda$):

$$\begin{aligned}
&{\rm ZGN}(\lambda) = \frac{Z_{500}(\lambda,\phi_{\rm N}) - Z_{500}(\lambda,\phi_0)}{\phi_{\rm N} - \phi_0} < -10 ,\\
&{\rm ZGS}(\lambda) = \frac{Z_{500}(\lambda,\phi_0) - Z_{500}(\lambda,\phi_{\rm S})}{\phi_0 - \phi_{\rm S}} > 0 ,\\
&Z_{500}(\lambda,\phi_0) - \overline{Z_{500}(\lambda,\phi_0)} > 0 ,
\end{aligned} \tag{1}$$

where

$$\begin{aligned}
\lambda &\in [0, 357.5] ,\\
\phi_{\rm N} &= 80°{\rm N} + \Delta ,\\
\phi_0 &= 60°{\rm N} + \Delta ,\\
\phi_{\rm S} &= 40°{\rm N} + \Delta ,\\
\Delta &= -5, -2.5, 0, 2.5 \text{ or } 5 .
\end{aligned}$$

Based on previous climatological studies, the central reference point ($\phi_0$) was chosen as 60°N (Austin, 1980; Lejenäs and Øakland, 1983) while the northern and southern points were set at 80°N and 40°N (Tibaldi and Molteni, 1990). Because the north–south position of the blocking high center varies with season and geographic region (Pelly and Hoskins, 2003; Barriopedro et al., 2006), a fluctuation of 5° latitude was accepted (Barriopedro et al., 2006), which is denoted by $\Delta$. This can overcome the one-dimensional constraint of the blocking index proposed by Tibaldi and Molteni (1990). A longitude grid point is said to be blocked (called blocking longitude) when the three criteria in Eq. (4) are simultaneously satisfied by at least one of the five latitude pairs (e.g., $\phi_{\rm N}$, $\phi_0$, $\phi_{\rm S}$).

Because blocking is at least of synoptic scale, a blocking region should be composed of minimum number of blocking longitudes that are comparable to this scale. In this study, a blocking region on one day has to consist of at least five consecutive blocking grid points (i.e., 12.5° longitude). Unlike previous studies (e.g., Barriopedro et al., 2006), there is no non-blocking longitude inside any blocking region. After detecting the blocking regions, the characteristics of each region are quantified. First, the westernmost and easternmost blocking longitudes of the region ($\lambda_{\rm w}$, $\lambda_{\rm e}$) are recorded and the distance between the two longitudes is taken as the extension. Second, the center of the region corresponds to the latitude and longitude with maximum meridional-averaged and zonal-averaged geopotential height value. The average is taken as the ensemble mean of all grid points along the side within the blocking region. As mentioned in Barriopedro et al. (2006), sometimes the relative high center is not inside the blocking region (e.g., due to tilting of the blocking ridge). Thus, the longitude is better when extending 5° to the west of the grid point $\lambda_{\rm w}$ or east of the grid point $\lambda_{\rm e}$. Third, after identifying the blocking high center, an instantaneous intensity for a blocking region is measured by the following blocking index (BI):

$${\rm BI} = 100.0[Z_{500}(\lambda,\phi)/Z_{\rm reef} - 1.0] ,$$

where

$$Z_{\rm reef} = [Z_{500}(\lambda_{\rm up},\phi) + Z_{500}(\lambda_{\rm down},\phi)]/2 , \tag{2}$$

$\lambda_{\rm up}$ and $\lambda_{\rm down}$ are the upstream and downstream longitude grid points at the half-extension from the center longitude grid point of the blocking region.

The final procedure of the detection algorithm is to determine the duration of a blocking event. Choosing the threshold duration for a blocking event was arbitrary in previous works, which varied from 3 days (Elliot and Smith, 1949) to 30 days (Trieidl et al., 1981). However, the selection of this value may be deterministic for interpreting our results. Considering the characteristic time of blocking regions of all durations (Pelly and Hoskins, 2003), it is adequate to choose four days as the minimum duration of a blocking event. The length is close to the characteristic length of persistent height anomalies, which is ∼five days, as determined by Dole and Gordon (1983). In addition, the

[a]Blocking Index website in the Climate Prediction Center (CPC) of NOAA: http://www.cpc.ncep.noaa.gov/products/precip/CWlink/blocking/index/index.nh.shtml

intensity and extension of a blocking event is taken as the largest BI and the mean of all daily extension, respectively, throughout its lifetime.

## 3. Northern Hemisphere blocking frequency

The longitudinal distribution of the median, as well as the 25th, 75th, and 95th percentiles of the Northern Hemisphere blocking frequency in four seasons for the period 1950–2009 are shown in Fig. 1. The distributions were only composed of the blocking regions that persisted for at least four days. Those instantaneous blocking regions persisting for less than four days were excluded. Generally, there are two major blocking sectors over the eastern Atlantic Ocean–European Continent (Euro–Atlantic sector) and the Pacific Ocean (Pacific sector). Their boundaries, signified by minimum blocking frequencies, were identified at the Asian continent (∼90°E) and the American continent (∼90°W) over which the Tibetan Plateau and the Rocky Mountains are located, respectively. The Euro–Atlantic sector had the highest hemispheric blocking frequency, with a prominent peak over the European continent (∼0°–30°E), especially in spring and autumn. In summer, there was also a peak near the Ural Mountains (∼60°E), which is the third major blocking region, as mentioned in the introduction. On the other hand, the Pacific sector attained its highest frequency in winter, which was comparable to its Atlantic counterpart. Its activity reached a peak near the central Pacific in winter and spring, whereas in summer there were two peaks over the Sea of Okhotsk (∼140°E) and Alaska (∼150°W). Moreover, the activity over the entire Pacific sector was quite low, with a mean of <1 day in autumn. Overall, the ratio of the peak of the Euro–Atlantic sector to that of the Pacific sector was 1.7.

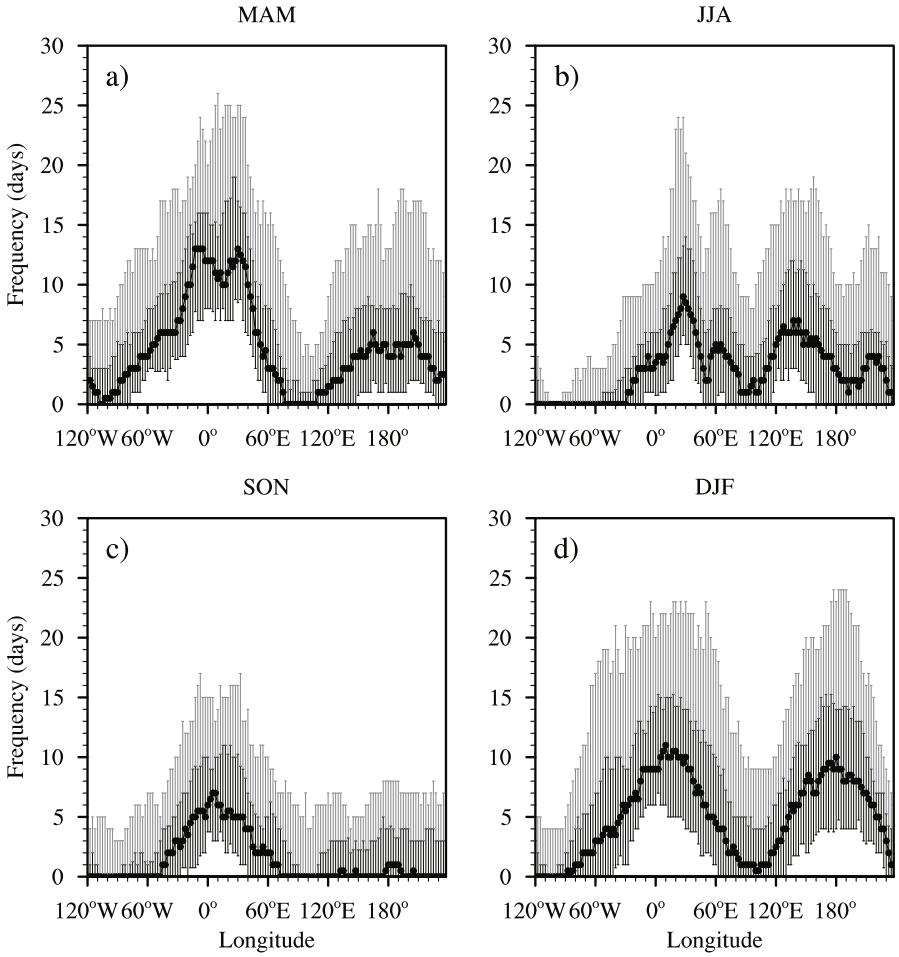


**Fig. 1.** The 60-yr climatology of the frequency of blocking in the Northern Hemisphere blocking in four seasons as a function of longitude: (a) spring (MAM), (b) summer (JJA), (c) autumn (SON) and (d) winter (DJF), where the solid line indicates the median, black error bars denote the 25th and 75th percentiles, and gray error bars denote the 75th and 95th percentiles. Units: d.

All of these results were consistent with those reported by Wiedenmann et al. (2002) and Barriopedro et al. (2006). The major climatological features of the blocking frequency distribution were also similar to those found using other detection methods, such as Diao et al. (2006) and Tyrlis and Hoskins (2008a).

The climatological pictures of Northern Hemisphere blocking frequency (Fig. 1) indicate that blocking rarely persisted over the East Asian continent, especially in the transition periods (Figs. 1a and c). Apparently, the impact of blocking on East Asia was contributed mainly by its upstream or downstream cyclonic vortex rather than its center. The geographic origins of blocking can be deduced according to Fig. 2. Figure 2 illustrates the averaged first-detected and last-detected positions of blocking events, known as the genesis and decay positions. A higher genesis frequency at one longitude grid point suggests that the blocking events tended to recede there, while a higher decaying frequency suggests that the blocking events tended to approach. The blocking from the Ural Mountains and the Western Pacific exerted a high impact on East Asia, except in summer where the blocking formed more frequently over the Asian continent. Accordingly, the impact of blocking events on East Asia was studied according to three groups of events, each spanning 42.5° longitude: (A) Ural-Siberia: 45.0°–87.5°E; (B) East Asia: 90.0°–132.5°E and (C) Western Pacific: 135.0°–177.5°E.

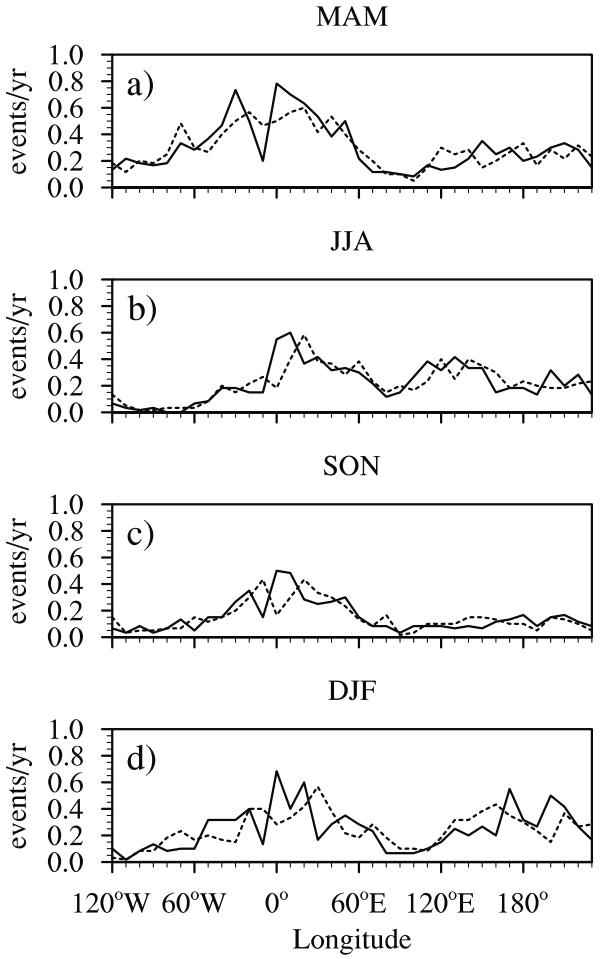


**Fig. 2.** Averaged genesis (solid) and decaying (dashed) locations of blocking events in four seasons as a function of longitude. Units: $yr^{-1}$.

## 4. Winter blocking

In the boreal winter, blocking often moves as if a quasi-stationary Rossby wave packet propagates eastward over Eurasia (Nakamura et al., 1997; Takaya and Nakamura, 2005). As shown in Fig. 2d, there were two major formation centers over Eurasia, with a primary peak over Scandinavia (∼20°–30°E) and a secondary peak upstream of the Ural Mountains (∼50°–60°E). The recurrence of blocking events over these two regions was analogous to the two major blocking patterns over Ural–Siberia identified by Cheung et al. (2012a). They suggested that the blocking persisting over the latter (former) region corresponded to a uniform (opposite) sign of the temperature anomaly pattern in the northern and southern part of the EAWM. while the blocking persisting over the former region corresponded to an opposite sign of temperature anomaly pattern. On the other hand, the blocking formed over the Western Pacific and Central Pacific often took a westward path. Such movement characterizes the westward propagating Rossby wave identified by Lau and Nath (1999). Basically, these results confirm the results of Takaya and Nakamura (2005), where the impact of blocking on East Asian cold surges was exerted by the events originating upstream and downstream of the quasi-stationary East Asian trough.

Figure 3 shows the evolution of three groups of blocking events defined in section 3. The blocking formation over Ural–Siberia (left panel in Fig. 3) is followed by the intensification of the East Asian jet stream. The southeastward migration of the positive anomaly of 300-hPa zonal wind from day zero to day four resembles a cold air outbreak in East Asia (Wu and Chan, 1997). This suggests an intensification of the jet stream following the development of a cold Siberian high. On the other hand, the blocking from the Western Pacific is accompanied by a southeastward shift of the East Asian jet stream (middle panel in Fig. 3). It does not show a dynamic linkage with the Siberian high as the Ural–Siberian event does, and hence it exerts a relatively weak impact on the general

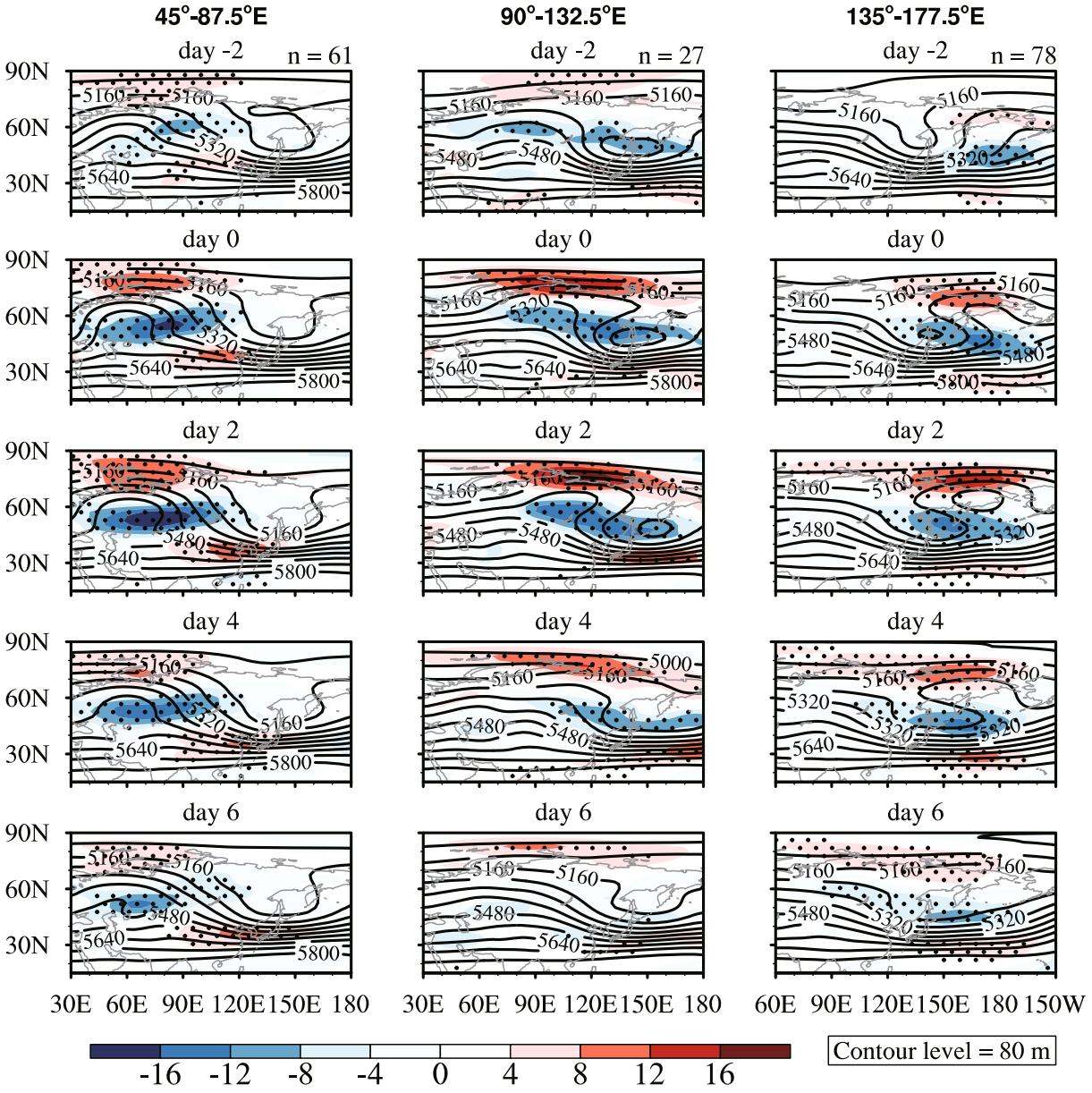


**Fig. 3.** Lagged composites of wintertime (DJF) blocking events formed over Ural–Siberia (left panel), East Asia (middle panel) and Western Pacific (right panel) from day −2 to day 6 relative to their establishment (day 0): 500-hPa geopotential height (contour; units: m) and 300-hPa zonal wind anomaly (shading; units: m $s^{-1}$). The dotted area indicates that the 300-hPa zonal wind is significantly different from the climatological mean during the same period between 1950 and 2009 at the 99% confidence level based on a two-tailed Student's t-test.

circulation over East Asia. In addition, there are few blocking events formed over East Asia (27 out of 166 events, 16.3%). Their formation was characterized by the northeastward extension of a blocking ridge and the deepening of the East Asian trough (Fig. 3, right panel). Due to the small proportion of East Asian blocking compared to the number of the other two groups, the blocking over Ural–Siberia should be of primary concern for studying its impact on the East Asian winter climate. Indeed, the frequent occurrence of this group of blocking events was responsible for triggering extreme weather and climate in East Asia, such as long-lasting cold periods in January–February 1984 (Bueh et al., 2011), February–March 2005 (Lu and Chang, 2009), and January–February 2008 (Zhou et al., 2009).

## 5. Summer blocking

In the boreal summer, the warmer continent supports the formation and persistence of more blocking over Eurasia, especially East Asia (79 out of 217 events

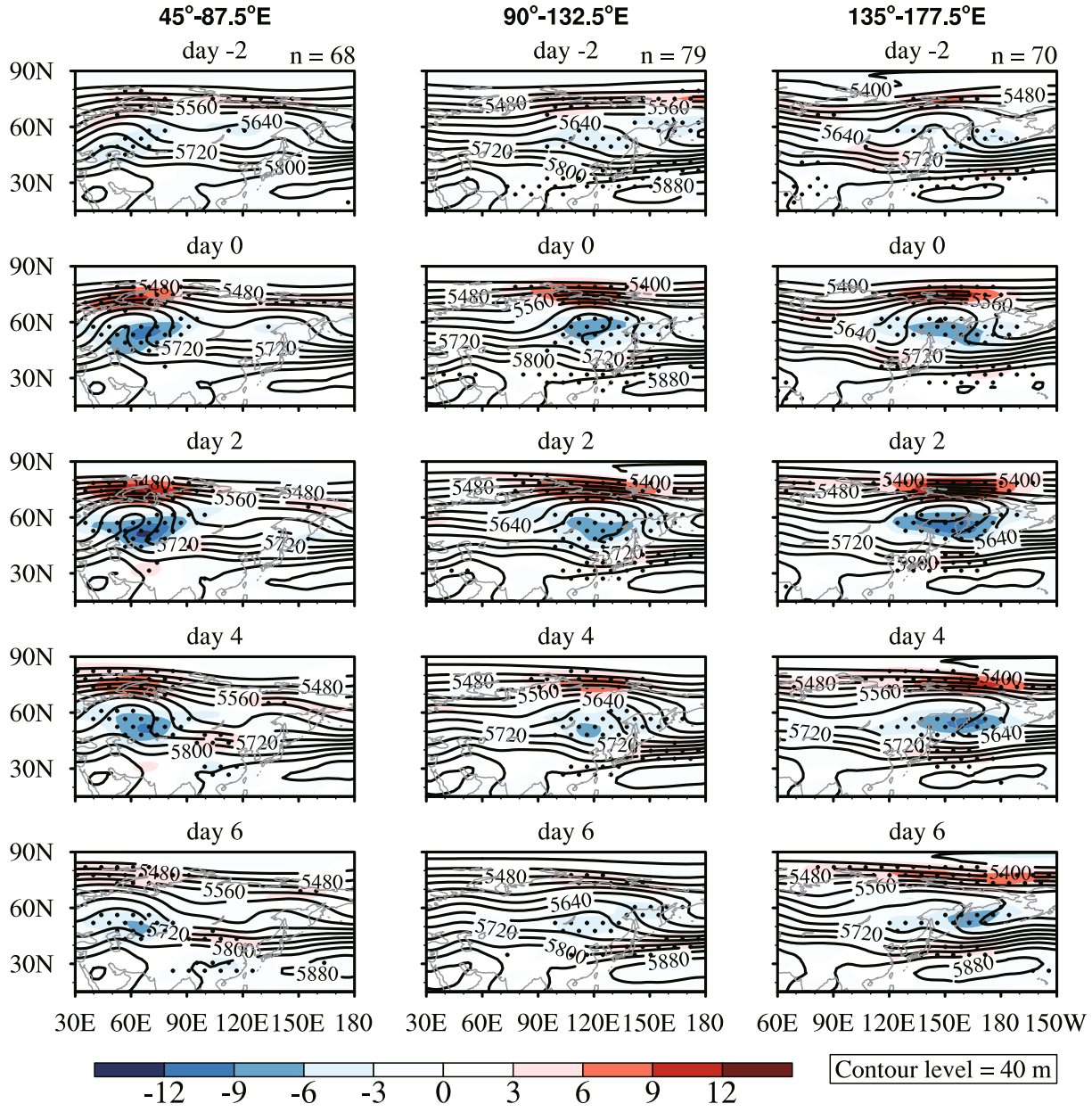


**Fig. 4.** Same as Fig. 3, but for summertime (JJA) blocking events.

= 36.4%, c.f. 16.3% in winter). Generally, the impact of three groups of summer blocking (Fig. 4) was not as intense and extensive as that in winter (Fig. 3). During the formation of Ural–Siberian blocking, it was associated with an intensification of the jet stream to its southeast in winter (day zero in the left panel of Fig. 3). In summer, however, the zonal wind anomaly to its downstream was not pronounced until day four (left panel of Fig. 4). It appears that Ural–Siberian blocking exerted a strong impact on East Asia when it moved eastward over the Asian continent, which was similar to the findings of Li and Ding (2004). On the other hand, the wind anomalies associated with Asian and Western Pacific blocking in summer extended southward to a lesser extent than those in winter. This weaker impact may have arisen from the difference in the thermodynamic background between the two seasons. Because of a warmer continent in summer, the thermal contrast, as well as the pressure gradient, between the center of blocking and its upstream and downstream side was smaller than in winter. The impact can also be measured by the temporal features of individual blocking event; their climatology in different seasons is presented in the next section.

**Table 1.** Annually and seasonally climatological mean and standard deviation of temporal characteristics of blocking events.

| | Annual | Spring (MAM) | Summer (JJA) | Autumn (SON) | Winter (DJF) |
|---|---|---|---|---|---|
| Number of events | 1937 | 616 (31.8%) | 483 (24.9%) | 325 (16.8%) | 513 (26.5%) |
| Duration (d) | 6.21±2.70 | 6.09±2.50 | 6.04±2.79 | 6.05±2.36 | 6.58±2.99 |
| Intensity | 4.09±1.85 | 4.14±1.64 | 2.84±1.06 | 3.95±1.57 | 5.25±2.06 |
| Extension (°) | 29.8±10.5 | 29.6±10.1 | 26.1±8.07 | 26.9±8.00 | 35.2±12.1 |

## 6. Characteristics of blocking

The characteristics of blocking events and their seasonality are summarized in Table 1. There were 1937 events for the entire study period, giving rise to an annually-averaged number of 32. The number is higher than that identified by some previous works (e.g., 22 by Watson and Colucci, 2002; 25 by Barriopedro et al., 2006) because of smaller number of days of the persistence criterion. The hemispheric blocking activity is higher in spring and lower in autumn. The intensity and extension attained a maximum in winter and a minimum in summer, which is similar to earlier findings of Lupo and Smith (1995) and Wiedenmann et al. (2002). Moreover, Table 1 also suggests that the duration exhibited weak changes among four seasons and was close to a week (∼five days), which is consistent with previous studies (e.g., Tyrlis and Hoskins, 2008a). However, the hemispheric means may have smoothed out the regional characteristics of blocking. In the past, most studies have presented the regional characteristics by comparing the quantities among some fixed regions (e.g., Wiedenmann et al., 2002; Barriopedro et al., 2006). Due to the availability of 60-year reanalysis datasets, we were able to obtain sufficient samples of blocking to make up the longitudinal distribution of each characteristic to make the comparisons (Figs. 5–7).

The quantity at every longitude of each line was taken as the average of that quantity of all days in a given season with blocking over that longitude (Figs. 5–7). These figures emphasize the spatial variation of each temporal feature. The seasonal variation of the duration of blocking was most remarkable over the Atlantic sector, which is longer in winter (∼10 days) and shorter in summer (∼six days) (Fig. 5). The duration was a local maximum near the Ural Mountains where the seasonal variation was not strong, which suggests that the blocking tended to persist there in all seasons. On the other hand, the intensity of blocking was generally higher over the open ocean and is lower over the continent except in summer (Fig. 6). This is partially related to the zonal temperature gradient, which was enhanced by the land–sea thermal contrast in winter. Because part of the block-

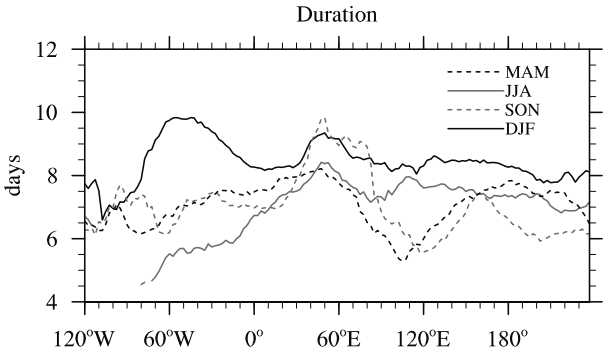


**Fig. 5.** The duration of blocking events over the Northern Hemisphere in four seasons as a function of longitude, where the longitudes of <20 blocking events are represented by broken lines.

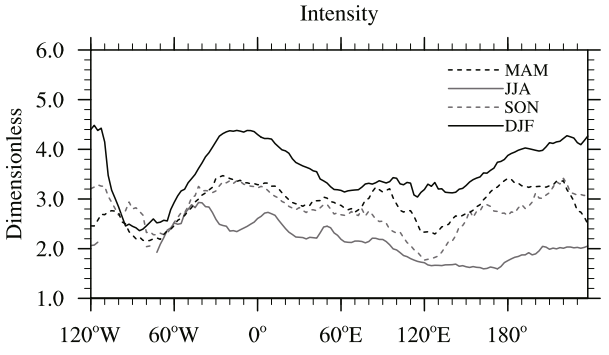


**Fig. 6.** Same as Fig. 5, but for the intensity of blocking events.

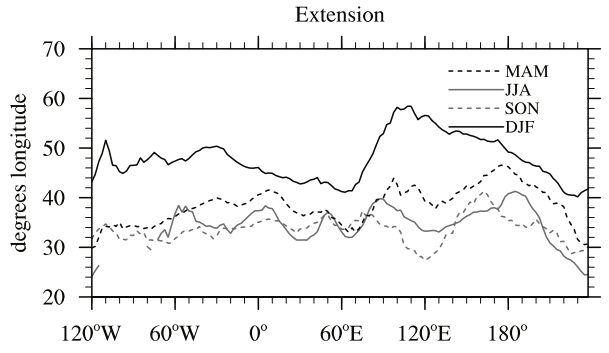


**Fig. 7.** Same as Fig. 5, but for the extension of blocking events.

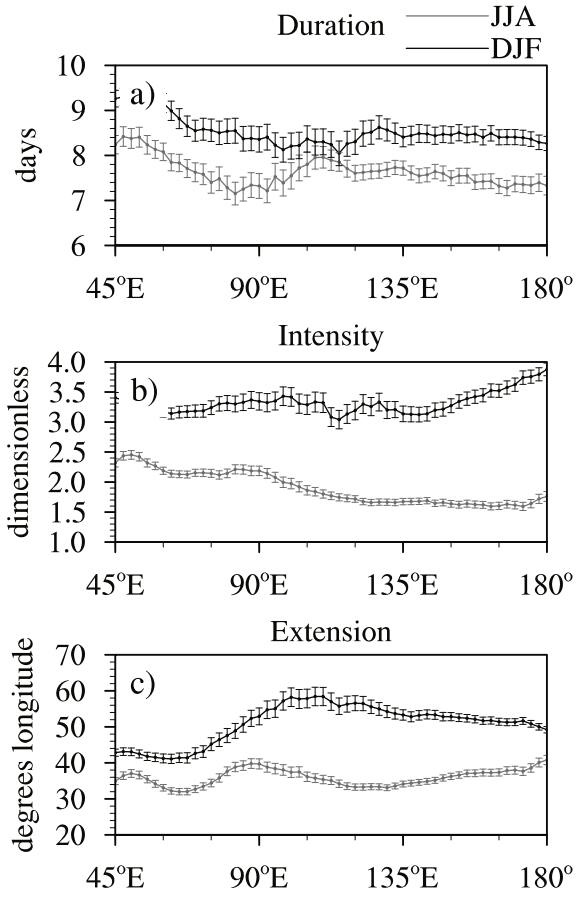


**Fig. 8.** The mean (solid line) and standard error (error bar) of the temporal characteristics of blocking events between 45°E and 180° in summer (gray) and winter (black): (a) duration, (b) intensity, and (c) extension.

ing moved eastward across Europe from the Atlantic Ocean, the intensity of such oceanic blocking event may have decreased tremendously over Europe. Moreover, the blocking over Asia is formed locally or migrated from the west near the Ural Mountains. This was a continental blocking event and hence its intensity remained fairly constant.

Unlike the intensity, the extension of blocking did not exhibit a strong spatial variation over the Western Hemisphere (Fig. 7). Interestingly, it was much higher over East Asia (∼90°E) in winter. The blocking occurrence attained a minimum over this region, where the climatological quasi-stationary trough was located (Figs. 1d and 2d). By comparing the extension to the east and west of East Asia, it can be deduced that the higher blocking extension over this region in winter was mainly due to the westward extension of Pacific blocking. In contrast, the extension over East Asia was comparable with both Ural–Siberia and Western Pacific in summer because more blocking formed locally.

**Table 2.** Correlation matrix for the temporal characteristics of blocking events.

| Correlation | Duration (d) | Intensity | Extension (°) |
|---|---|---|---|
| Duration (d) | | 0.342 | 0.242 |
| Intensity | 0.342 | | 0.462 |
| Extension (°) | 0.242 | 0.462 | |

Even though the intensity and extension had different spatial distributions in winter, both displayed very strong seasonal variation across most of the Northern Hemisphere (Figs. 6 and 7). Figure 8 shows the standard errors, as well as the means, of the three temporal characteristics over every longitude grid point in our domain of interest. Except for the duration over East Asia, all of these characteristics were significantly different between summer and winter. The differences in extension and intensity were well above the 99% confidence level (not shown). Table 2 summarizes the correlation among different characteristics of blocking events. All linear correlation coefficients in the table are statistically significant at the 99% confidence level. Furthermore, Figure 9 clearly shows that the extension was directly proportional to the intensity. Such a strong linear relationship did not change with season (not shown); hence, we suggest that the physical mechanisms responsible for one of

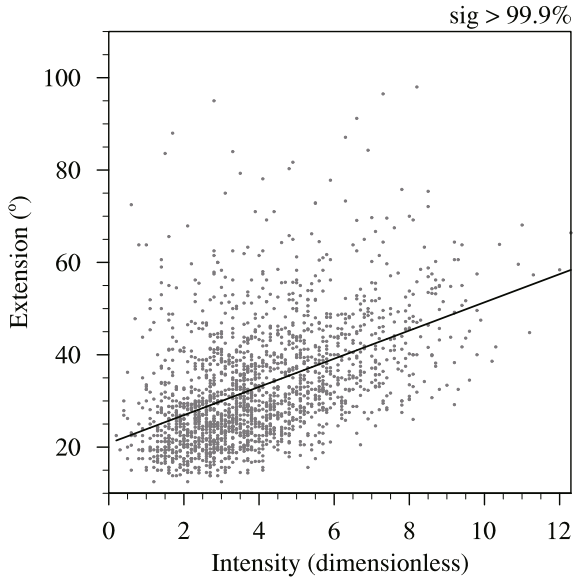


**Fig. 9.** A scatter plot between the intensity and the extension of blocking events. The linear regression between the two quantities found by the least-squares fit is denoted by the black solid line, and its confidence level is shown at the top right.

the blocking characteristics may be related to the others.

## 7. Discussion

Blocking formation is mainly attributed to intense cyclogenesis upstream prior to its development (e.g., Rex, 1950; Dole, 1986; Egger et al., 1986) following a rapidly developing surface cyclone (Colucci, 1985; Tsou and Smith, 1990; Alberta et al., 1991). Because explosive cyclogenesis usually occurs in winter and rarely in summer, it is discernible as the difference in blocking frequency and intensity between the two seasons (Lupo and Smith, 1995). In spite of different temporal and spatial scales of synoptic cyclones and blocking anticyclones, the two systems show dynamical linkages involving interactions between synoptic-scale eddies and planetary-scale waves (Frederiksen, 1982; Hansen and Chen, 1982; Dole and Gordon, 1983; Colucci, 1985; Luo et al., 2010a; Jiang and Wang, 2012). In an idealized case, blocking is identified as a manifestation of multiple equilibrium states that favors amplification of waves and development of weather systems (Charney and DeVore, 1979). Furthermore, Reinhold and Pierrehumbert (1982) found that blocking could form under the equilibrium between the synoptic-scale heat and momentum transport and the planetary waves. These studies were illustrated by an observational study by Colucci (1985), who found that cyclogenesis near the long-wave ridge and trough axis is favorable for the formation of blocking anticyclonic and cyclonic vortices, respectively. Due to the change in the spatial distribution of net solar radiation between summer and winter, the locations of jet stream and major ridges and troughs vary according to the thermal wind relationship. In short, in winter the cyclonic shear is dominant for the formation of oceanic blocking and the anticyclonic shear is dominant for the formation of continental blocking; the reverse is true in summer (Tyrlis and Hoskins, 2008b). This can also explain the preferred geographic location of blocking in the two seasons.

Because summer blocking is generally of lower intensity and smaller extension compared to winter blocking, a single summer blocking event makes a less pronounced impact on East Asia, as shown in section 5. In winter, a severe cold surge is often initiated after the decay of Ural–Siberian blocking or Asian blocking, which may bring a large temperature drop to the majority of East Asia and enhance the convection over the tropical Pacific (Chang et al., 1979). In summer, on the other hand, the anomalous circulation associated

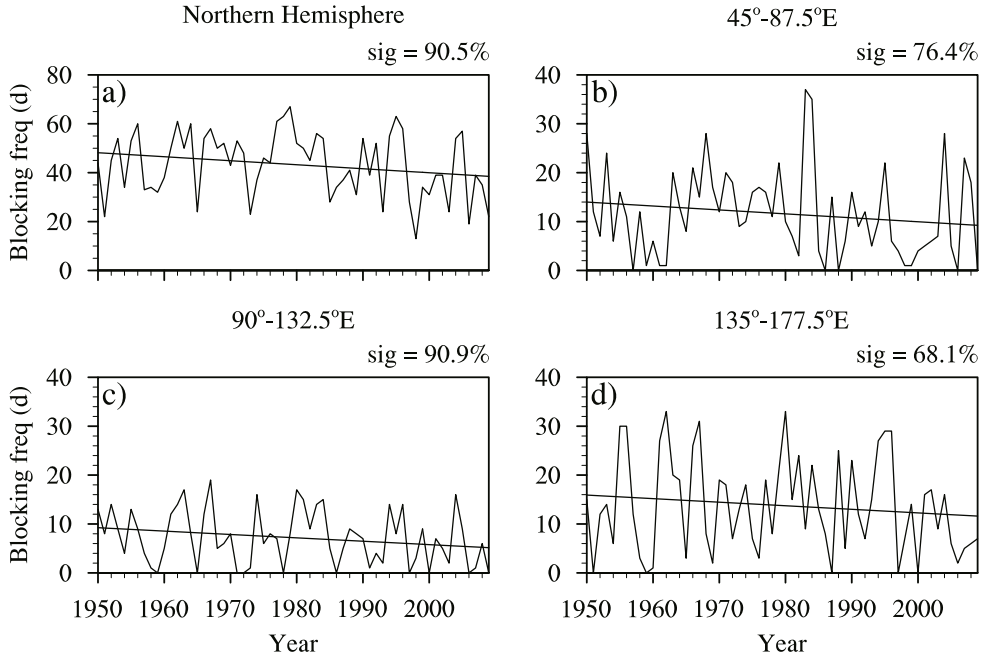


**Fig. 10.** Interannual time-series of the area-averaged blocking frequency over Ural–Siberia (solid black), East Asia (solid grey), and Western Pacific (dashed black) in winter (DJF) for the period 1950–2009. The three time series are all shown in panel (a), whereas each of the time series is also shown separately in panels (b) through (d), together with the linear regression line fitted by the least-squares fit, where the confidence level is shown at the top right.

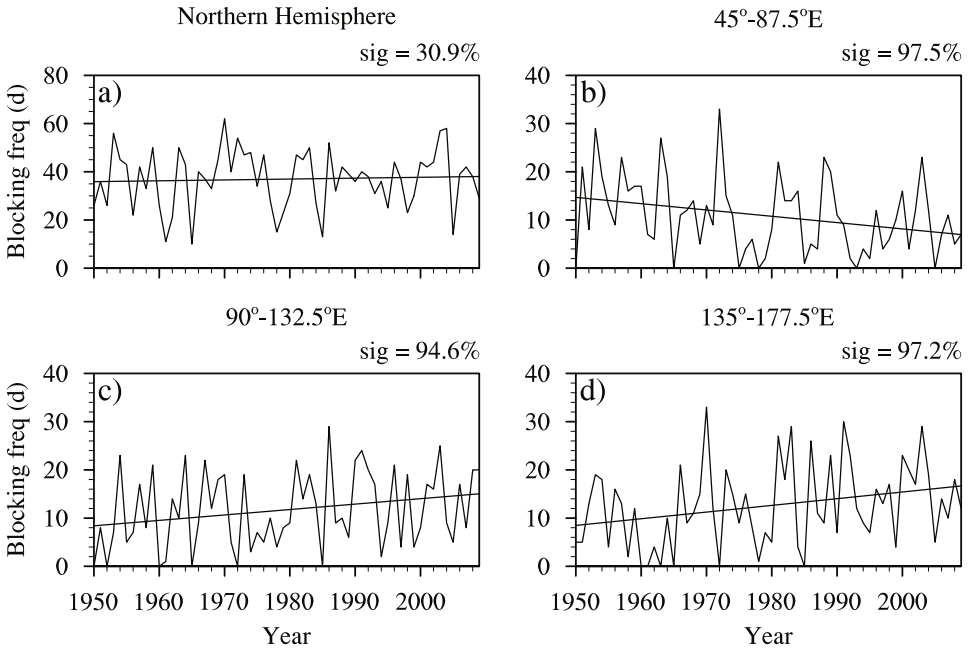


**Fig. 11.** Same as Fig. 9, but for summer (JJA).

with blocking is more confined to its center and downstream portion. Thus, the impact of Ural–Siberian blocking on East Asia is significant only when it persists for several days and moves toward East Asia. Furthermore, it generally does not exert a direct impact on the southern part (south of 30°N) as winter blocking does. However, because much more blocking forms over the Asian continent in summer, part of the midlatitude region, such as northeastern China and Japan, may be more frequently affected by blocking than in winter.

Moreover, the interannual time-series of the blocking frequency in summer and winter over the Northern Hemisphere and the three selected regions is given in Figs. 9–10. The winter hemispheric blocking exhibits decreasing frequency that just exceeds the 90% confidence level (Fig. 10a). There is no significant increasing or decreasing trend in our area of interest (Figs. 10b–d), where a trend in East Asia exceeding the 90% confidence level is not obvious at all (Fig. 10c). This result is slightly different from those of Wang et al. (2010), which showed a declining blocking activity over 30°–90°E for the period 1957/58–2001/02. However, the methods of our study, including the study period (1950/51–2009/10), the reference region (Ural–Siberia, 45°–90°E), and the detection of blocking, were different from their study. Indeed, the blocking activity over Ural–Siberia was generally low between late 1980s and early 2000s (Fig. 10b). Also, the high blocking activity in recent years contributed to a strong EAWM, for example, 2004/05 (Lu and Chang, 2009) and 2007/08 (Zhou et al., 2009). It is of interest to study whether there were any decadal variations of blocking activity that could be related to the decadal variations of EAWM, as mentioned by Zhou et al. (2007a, b), as well as that of austral summer rainfall in northeast Australia (Li et al., 2012)

On the other hand, there was no overall change in summer hemispheric blocking frequency (Fig. 11a). The summer blocking frequency over the Western Pacific (Ural–Siberia) underwent remarkable increasing and decreasing trends that exceeded the 95% confidence level (Figs. 11b, d). Therefore, the impact of summer blocking on East Asian circulation is noteworthy. Because the occurrence of summer blocking affects the meridional movement of the meiyu/baiu front (Wang, 1992), we are curious whether the increasing trend of summer blocking frequency was related to the southward shift of the East Asian summer monsoon components in the past few decades (Li et al., 2010). In addition, the long-term change of different temporal characteristics was not analyzed because of the limited number of blocking events in each year.

## 8. Summary

In this study, we reviewed the climatology of Northern Hemisphere blocking to investigate the possible impact of blocking on East Asia. Overall, the results are consistent with previous findings (e.g., Lupo and Smith, 1995; Barriopedro et al., 2006; Diao et al., 2006; Tyrlis and Hoskins, 2008a). The Atlantic

Ocean–European continent and the Pacific Ocean are the two major blocking sectors. Over Eurasia, the vicinity of the Ural Mountains is the preferred geographic location of blocking in every season. The strength of blocking events, in terms of intensity and extension, is stronger in winter and weaker in summer.

In winter, blocking events from the Ural–Siberia region potentially trigger considerable impact in East Asia by reinforcing the cold Siberian high. Even though frequent occurrences of Pacific blocking move westward toward East Asia, this group of blocking events does not interact with the Siberian high. Therefore, the occurrence of Ural–Siberian blocking is of primary concern for studying the impact of blocking on the circulation in East Asia. In summer, on the other hand, the blocking that forms over this region exerts a high impact on East Asia only if it moves toward East Asia. Apart from Ural–Siberian blocking, blocking episodes occur over Asia and the Sea of Okhotsk. Even though summer blocking is generally weaker and smaller, its persistence over East Asia and summer monsoon activities (e.g., Zhou et al., 2006) are likely to be associated with persistent anomalous circulation over the extratropical regions, which may be of increasing importance under the increasing trend of summer Western Pacific blocking.

The climatological information gleaned from this study is vital for studying the impact of blocking on East Asia. Particularly, it is important to analyze the physical and dynamical mechanisms responsible for different characteristics of blocking events, where the winter events in the vicinity of the Ural Mountains have been investigated by Han et al. (2011) and Cheung et al. (2012b). We are also curious whether the variability of blocking can explain that of East Asian summer and winter monsoon on different timescales.

***Acknowledgements.*** The authors would like to express the gratitude for the valuable comments provided by an anonymous reviewer. The work described in this paper was fully/partial supported by a grant from the Research Grants Council of the Hong Kong Special Administrative Region (Grant No. 104410) and a grant from Germany/Hong Kong Joint Research Scheme (Grant No. G_HK023/09). The figures were prepared by the NCAR Command Language (Version 6.0.0) [Software] (2012), Boulder, Colorado: UCAR/NCAR/CLSL/VETS.

## REFERENCES

Alberta, T. L., S. J. Colucci, and J. C. Davenport, 1991: Rapid 500 mb cyclogenesis and anticyclogenesis. *Mon. Wea. Rev.*, **119**, 1186–1204.

Anderson, J. L., 1993: The climatology of blocking in a numerical forecast model. *J. Climate*, **6**, 1041–1056.

Austin, J. F., 1980: The blocking of mid-latitude westerly wind by planetary waves. *Quart. J. Roy. Meteor. Soc.*, **106**, 327–350.

Barriopedro, D., R. García-Herrera, A. R. Lupo, and E. Hernandez, 2006: A climatology of Northern Hemisphere blocking. *J. Climate*, **19**, 1042–1063.

Barriopedro, D., R. García-Herrera, and R. M. Trigo, 2010: Application of blocking diagnosis methods to general circulation models. Part I: A novel detection scheme. *Climate Dyn.*, **35**, 1373–1391.

Bueh, C., N. Shi, and Z. Xie, 2011: Large-scale circulation anomalies associated with persistent low temperature over southern China in January 2008. *Atmos. Sci. Lett.*, **12**, 273–280.

Chang, C.-P., J. E. Erickson, and K. M. Lau, 1979: Northeasterly cold surges and near-equatorial disturbances over the winter MONEX area during December 1974. Part I: Synoptic Aspects. *Mon. Wea. Rev.*, **107**, 812–829.

Charney, J. G., and J. G. DeVore, 1979: Multiple flow equilibria in the atmosphere and blocking. *J. Atmos. Sci.*, **36**, 1205–1216.

Chen, W., S. Yang, and R.-H. Huang, 2005: Relationship between stationary planetary wave activity and the East Asian winter monsoon. *J. Geophys. Res.*, **110**, D14110, doi: 10.1029/2004JD005669.

Cheung, H. N., W. Zhou, H. Y. Mok, and M. C. Wu, 2012a: Relationship between Ural-Siberian blocking and the East Asian winter monsoon in relation to the Arctic Oscillation and El Niño-Southern Oscillation. *J. Climate*, **25**, 4242–4257.

Cheung, H. N., W. Zhou, Y. Shao, W. Chen, H. Y. Mok, and M. C. Wu, 2012b: Observational climatology and characteristics of wintertime atmospheric blocking over Ural–Siberia. *Climate Dyn.*, doi: 10.1007/s00382-012-1587-6. (in press)

Colucci, S. J., 1985: Explosive cyclogenesis and large-scale circulation changes: Implications for atmospheric blocking. *J. Atmos. Sci.*, **42**, 2701–2717.

Diao, Y., J. Li, and D. Luo, 2006: A new blocking index and its application: Blocking action in the Northern Hemisphere. *J. Climate*, **19**, 4819–4839.

Dole, R. M., 1986: The life cycles of persistent anomalies and blocking over the North Pacific. *Advances in Geophysics*, **29**, 31–70.

Dole, R. M., and N. D. Gordon, 1983: Persistent anomalies of the extratropical Northern Hemisphere wintertime circulation: Geographical distribution and regional persistence characteristics. *Mon. Wea. Rev.*, **111**, 1567–1586.

Dole, R. M., and Coauthors, 2011: Was there a basis for anticipating the 2010 Russian heat wave? *Geophys. Res. Lett.*, **38**, L06072, doi: 10.1029/2010GL046582.

Egger, J., W. Metz, and G. Müller, 1986: Forcing of planetary-scale blocking anticyclones by synoptic-scale eddies. *Advances in Geophysics*, **29**, 183–198.

Elliot, R. D., and T. B. Smith, 1949: A study of the effects of large blocking highs on the general circulation in the northern-hemisphere westerlies. *J. Meteor.*, **6**,

67–85.

Frederiksen, J. S., 1982: A unified three-dimensional instability theory of the onset of blocking and cyclogenesis. *J. Atmos. Sci.*, **39**, 969–987.

Han, Z., S. L. Li, and M. Mu, 2011: The role of warm North Atlantic SST in the formation of positive height anomalies over the Ural Mountains during January 2008. *Adv. Atmos. Sci.*, **28**, 246–256, doi: 10.1007/s00376-010-0069-1.

Hansen, A. P., and T.-C. Chen, 1982: A spectral energetic study of atmospheric blocking. *Mon. Wea. Rev.*, **110**, 1146–1165.

Hong, C.-C., H.-H. Hsu, H.-H. Chia, and C.-Y. Wu, 2008: Decadal relationship between the North Atlantic Oscillation and cold surge frequency in Taiwan. *Geophys. Res. Lett.*, **35**, L24707, doi: 10.1029/2008GL034766.

Huang, R. H., J. L. Chen, L. Wang, and Z. D. Lin, 2012: Characteristics processes, and causes of the spatio-temporal variabilities of the East Asian monsoon system. *Adv. Atmos. Sci.*, **29**, 910–942, doi: 10.1007/s00376-012-2015-x.

Hung, C., and P. Kao, 2010: Weakening of the winter monsoon and abrupt increase of winter rainfalls over northern Taiwan and southern China in the early 1980s. *J. Climate*, **23**, 2357–2367.

Jiang, Z. N., and D. H. Wang, 2012: The behaviors of optimal precursors during wintertime Eurasian blocking onset. *Adv. Atmos. Sci.*, **29**, 1174–1184, doi: 10.1007/s00376-012-1102-3.

Kalnay, E., and Coauthors, 1996: The NCEP/NCAR 40-year reanalysis project. *Bull. Amer. Meteor. Soc.*, **77**, 437–471.

Lau, N. C., and M. J. Nath, 1999: Observed and GCM-simulated westward-propagating, planetary-scale fluctuations with approximately three-week periods. *Mon. Wea. Rev.*, **127**, 2324–2345.

Lau, W. K. M., and K.-M. Kim, 2012: The 2010 Pakistan flood and Russian heat wave: Teleconnection of hydrometeorologic extremes. *Journal of Hydrometeorology*, **13**, 392–403.

Lejenäs, H., and H. Økland, 1983: Characteristics of Northern Hemisphere blocking as determined from long time series of observational data. *Tellus*, **35A**, 350–362.

Li, F., and Y. Ding, 2004: Statistical characteristic of atmospheric blocking in the Eurasia high-mid latitudes based on recent 30-year summers. *Acta Meteorologica Sinca*, **62**, 347–354. (in Chinese)

Li, J., Z. Wu, Z. Jiang, and J. He, 2010: Can global warming strengthen the East Asian summer monsoon? *J. Climate*, **23**, 6696–6705.

Li, J., J. Feng, and Y. Li, 2012: A possible cause of decreasing summer rainfall in northeast Australia. *Int. J. Climatol.*, **32**, 995–1005, doi: 10.1002/joc.2328.

Lu, M.-M., and C.-P. Chang, 2009: Unusual late-season cold surges during the 2005 Asian winter monsoon: Roles of Atlantic blocking and the Central Asian anticyclone. *J. Climate*, **22**, 5205–5217.

Luo, D., J. T. Liu, and J. P. Li, 2010a: Interaction between planetary-scale diffluent flow and synoptic-scale waves during the life cycle of blocking. *Adv. Atmos. Sci.*, **27**, 807–831, doi: 10.1007/s00376-009-9074-7.

Luo, D., W. Zhou, and K. Wei, 2010b: Dynamics of eddy-driven North Atlantic Oscillations in a localized shifting jet: Zonal structure and downstream blocking. *Climate Dyn.*, **34**, 73–100.

Lupo, A. R., and P. J. Smith, 1995: Climatological features of blocking anticyclones in the Northern Hemisphere. *Tellus*, **47A**, 439–456.

Matsueda, M., 2011: Predictability of Euro-Russian blocking in summer of 2010. *Geophys. Res. Lett.*, **38**, L06801, doi: 10.1029/2010GL046557.

Nakamura, H., M. Nakamura, and J. L. Anderson, 1997: The role of high- and low-frequency dynamics in blocking formation. *Mon. Wea. Rev.*, **125**, 2074–2093.

Pelly, J. L., and B. J. Hoskins, 2003: A new perspective on blocking. *J. Atmos. Sci.*, **60**, 743–755.

Reinhold, B. B., and R. J. Pierrehumbert, 1982: Dynamics of weather regimes: Quasi-stationary waves and blocking. *Mon. Wea. Rev.*, **110**, 1105–1145.

Rex, D. F., 1950: Blocking action in the middle troposphere and its effect upon regional climate. I. An aerological study of blocking action. *Tellus*, **2**, 196–211.

Takaya, K., and H. Nakamura, 2005: Geographical dependence of upper-level blocking formation associated with intraseasonal amplification of the Siberian high. *J. Atmos. Sci.*, **62**, 4441–4449.

Tao, S., 1957: A synoptic and aerological study on a cold wave in the Far East during the period of the breakdown of the blocking situation over Euroasia and Atlantic. *Acta Meteorologica Sinica*, **35**, 155–165. (in Chinese)

Tibaldi, S., and F. Molteni, 1990: On the operational predictability of blocking. *Tellus*, **42A**, 343–365.

Treidl, R. A., E. C. Birch, and P. Sajecki, 1981: Blocking action in the Northern Hemisphere: A climatological study. *Atmos.-Ocean*, **19**, 1–23.

Tsou, C.-H., and P. J. Smith, 1990: The role of synoptic/planetary-scale interactions during the development of a blocking anticyclone. *Tellus*, **42A**, 174–193.

Tyrlis, E., and B. J. Hoskins, 2008a: Aspects of a Northern Hemisphere atmospheric blocking climatology. *J. Atmos. Sci.*, **65**, 1638–1652.

Tyrlis, E., and B. J. Hoskins, 2008b: The morphology of Northern Hemisphere blocking. *J. Atmos. Sci.*, **65**, 1653–1665.

Wang, L., W. Chen, W. Zhou, and R. Huang, 2009: Interannual variations of East Asian trough axis at 500 hPa and its association with the East Asian winter monsoon pathway. *J. Climate*, **22**, 600–614.

Wang, L., W. Chen, W. Zhou, J. C. L. Chan, D. Barriopedro, and R. Huang, 2010: Effect of the climate shift around mid-1970s on the relationship between

wintertime Ural blocking circulation and East Asian climate. *Int. J. Climatol.*, **30**, 153–158.

Wang, Y., 1992: Effects of blocking anticyclones in Eurasia in the rainy season (Meiyu/Baiu Season). *J. Meteor. Soc. Japan*, **70**, 929–951.

Watson, J. S., and S. J. Colucci, 2002: Evaluation of ensemble predictions of blocking in the NCEP global spectral model. *Mon. Wea. Rev.*, **130**, 3008–3021.

Wei, K., W. Chen, and W. Zhou, 2011: Changes in the East Asian cold season since 2000. *Adv. Atmos. Sci.*, **28**, 69–79, doi: 10.1007/s00376-010-9232-y.

Wiedenmann, J. M., A. R. Lupo, I. I. Mokhov, and E. Tikhonova, 2002: The climatology of blocking anticyclones for the Northern and Southern Hemispheres: Block intensity as a diagnostic. *J. Climate*, **15**, 3459–3473.

Woollings, T., B. J. Hoskins, M. Blackburn, and P. Berrisford, 2008: A new Rossby wave-breaking interpretation of the North Atlantic Oscillation. *J. Atmos. Sci.*, **65**, 609–626.

Wu, M. C., and J. C. L. Chan, 1997: Upper-level features associated with winter monsoon surges over South China. *Mon. Wea. Rev.*, **125**, 317–340.

Zhou, W., C. Y. Li, and J. C. L. Chan, 2006: The interdecadal variations of the summer monsoon rainfall over South China. *Meteor. Atmos. Phys.*, **93**, 165–175.

Zhou, W., C. Li, and X. Wang, 2007a: Possible connection between Pacific oceanic interdecadal pathway and East Asian winter monsoon. *Geophys. Res. Lett.*, **34**, L01701, doi: 10.1029/2006GL027809.

Zhou, W., X. Wang, T. Zhou, C. Li, and J. C. L. Chan, 2007b: Interdecadal variability of the relationship between the East Asian winter monsoon and ENSO. *Meteor. Atmos. Phys.*, **98**, 283–293, doi: 10.1007/s00703-007-0263-6.

Zhou, W., J. C. L. Chan, W. Chen, J. Ling, J. G. Pinto, and Y. Shao, 2009: Synoptic-scale controls of persistent low temperature and icy weather over southern China in January 2008. *Mon. Wea. Rev.*, **137**, 3978–3991.